ISBN: 978-3-95450-206-6 doi:10.18429/JACoW-FLS2018-THA1WC01

COMPACT ARC COMPRESSOR FOR FEL-DRIVEN COMPTON LIGHT SOURCE AND ERL-DRIVEN UV FEL*

S. Di Mitri, †, Elettra – Sincrotrone Trieste S.C.p.A., 34149 Basovizza, Trieste, Italy
I. Akkermans, I. Setjia, ASML Netherlands B.V. Technology, 5501 Veldhoven, The Netherlands
D. Douglas, Thomas Jefferson National Accelerator Facility, Newport News, VA 23606, USA
C. Pellegrini[1], SLAC National Accelerator Laboratory, Menlo Park, CA 94025, USA
G. Penn, M. Placidi (retired), Lawrence Berkely National Laboratory, Berkeley, CA 94720, USA
[1]also at University of California, Los Angeles, CA 90095, USA

Abstract

Many research and applications areas require photon sources capable of producing extreme ultra-violet (EUV) to gamma-ray beams with reasonably high fluxes and compact footprints. We explore the feasibility of a compact energy-recovery linac-driven EUV free electron laser (FEL), and of a multi-MeV gamma-rays source based on inverse Compton scattering from a high intensity UV FEL emitted by the electron beam itself. In the latter scenario, the same electron beam is used to produce gamma-rays in the 10-20 MeV range and UV radiation in the 10-15 eV range, in a ~4x22 m^2 footprint system.

MOTIVATIONS

This work recalls design strategies for the minimization of Coherent Synchrotron Radiation (CSR) instability [1] in high brightness electron beams time-compressed in compact multi-bend lattices, i.e., compressive arcs. Two examples are given: a compact Energy Recovery Linac (ERL)-driven Free-Electron Laser (FEL) for production of ~100 W average FEL power in EUV [2], and a compact FEL-driven Inverse Compton Scattering (ICS) light source devoted to geo-archaeology [3]. The ERL-FEL design targets a cost-effective method of producing integrated circuits and high-volume microchips through nano-lithography. The FEL-ICS design aims at the generation of ~10 MeV range photons in a compact footprint, for applications in computed tomography of cultural heritage and medical diagnostics.

COMPACT ERL–FEL

Overview

Figure 1 sketches a compact non-recirculating ERL-FEL, whose footprint is approximately 20x50 m^2. Table 1 lists the main parameters of the facility. The linear bunch length compression factor to be exploited in the arc is:

$$C = \frac{1}{|1+h_i R_{56}|} \approx \frac{1}{|1+\frac{\sigma_{\delta,i}}{\sigma_{z,i}} R_{56}|} \quad (1)$$

where h_i is the linear energy correlation with particle's longitudinal coordinate internal to the bunch, normalized to the beam mean energy (linear energy chirp), $\sigma_{\delta,i}$ and $\sigma_{z,i}$ are the rms relative energy spread and bunch length, respectively, all variables intended at the arc entrance; R_{56} is the linear transport matrix term proportional to the first order momentum compaction of the arc. The approximation in the r.h.s. of Eq.1 is valid as long as the total beam energy spread is dominated by the linear correlation term. Since the maximum FEL peak power is achieved for $\sigma_{\delta,i} <$ 0.1%, and given the initial 2 ps bunch length, a relatively large R_{56} is required in order to obtain a large compression factor, targeting the final peak current of 1 kA at the bunch charge of 100 pC. A large value for R_{56} implies a large energy dispersion function at the dipole magnets, and, in turn, a large CSR-induced projected emittance growth due to radiation emission and absorption in a dispersive region. Optics strategies to counteract such CSR effect are described in the following.

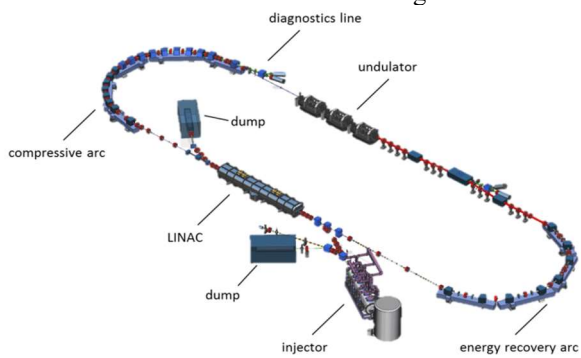

Figure 1: Conceptual scheme of an ERL-FEL; beam moves clock-wise. The scheme is not to scale, and a portion of the straight lines is omitted in order to make the arc lattice more evident. Copyright of APS.

Table 1: ERL-FEL Parameters

Parameter	Value	Unit
Bunch Charge	100	pC
Initial Bunch Duration	2.0	ps
Initial Proj. Norm. Emittance	0.5, 0.5	µm
Final Energy	1	GeV
Final Peak Current	1	kA
Final Relative Energy Spread	0.1	%
FEL Wavelength	13.5	nm
FEL Peak Power	1	GW
Arc Compression Factor	56	
Arc R_{56}	0.5	m
Proj. Norm. Emittance Growth	< 0.2	µm

* Work supported by Elettra Sincrotrone Trieste and ASML Netherlands B.V. Technology
† simone.dimitri@elettra.eu

ISBN: 978-3-95450-206-6 doi:10.18429/JACoW-FLS2018-THA1WC01

Arc Compressor

The impact of CSR kicks on the single particle's transverse momentum can be analytically calculated in the 1-D steady state approximation of CSR emission, for a longitudinal Gaussian charge distribution [4]. Assuming a localized kick and treating the magnet in thin lens approximation, the associated modification of the particle's transverse angular divergence in the dipole magnets and of its transverse position w.r.t. the reference dispersive trajectory can be analytically calculated assuming, e.g., a linear transport matrix formalism [2,5]. It is worth noticing that, since the bunch length is varying along the arc, the CSR kick at each dipole's location will depend on the bunch length at the entrance of the dipole, and therefore different kicks are expected along the arc even for identical optical functions at the magnets.

An analytical optimization of the Twiss parameters and of the betatron phase advance at the dipoles for the minimization of the cumulated CSR kick, and of the CSR-induced emittance growth, was given for a periodic arc compressor based on identical double-bend achromatic cells [6]. This solution, however, implies an arc length of at least 60 m at 1 GeV. Further reduction of the arc footprint is achieved as follows:

- the achromaticity condition at the end of each arc cell is relaxed, with the exception of the very last cell;
- the analytical prescription for the optimum value of Twiss parameters at each dipole (for minimum CSR kick) is relaxed, and strictly taken into account only in the very last cell, where largest CSR kicks are cumulated because of the shortest bunch duration;
- the two prescriptions above allow reducing the number of quadrupole magnets along the arc, leading to a more compact lattice. Eventually, a FODO-cell lattice is chosen, for a total arc length of 20 m;
- an optimization of the Twiss parameters and of the betatron phase advance for the cancellation of the cumulative CSR kick is carried out in the very last cell of the arc, where additional quadrupoles are inserted to this purpose.

The plot at the left side of Figure 2 shows the analytical prediction of the perturbation to the singe particle transverse coordinates at each dipole magnet, on the basis of the optics design illustrated in Fig.3. Figure 2-right plot shows an analytical prediction of emittance growth, based on the previous kicks calculation, as a function of the values of the Twiss parameters at the arc entrance. Such a scan allows a fine-tuning of the arc optics (which is no longer periodic, see Fig.3) once the quadrupole strengths are kept constant. The phase space diagram shows that most of the CSR kicks are relatively weak and lie in the upper-right side of the distribution. The last three kicks, instead, are larger in module and have opposite sign (both in x and x') respect to the others. Such a kicks configuration suggests the possibility of balancing the perturbations, thus providing a small global effect on the final beam emittance.

Particle tracking run with the `elegant` code [7], implementing 1-D CSR impedance and including transient CSR effects at the dipoles edges and in the drift sections, predicts a final projected normalized horizontal emittance of 0.73 μm rad, vs. the analytical prediction of 0.62 μm rad. No vertical emittance growth is predicted.

Second and third order transport matrix terms and CSR-induced nonlinear energy chirp contribute to distort the longitudinal beam phase space during the compression process. Nevertheless, an almost linear compression is obtained at the bunch head, where the current spike to 1 kA appears [2], by exploiting the leading linear energy chirp imparted by the CSR field [8]. An alternative and more complete linearization of the compression process would be possible with the insertion of sextupole magnets in the arc lattice [9], but at the expense of a longer beam line.

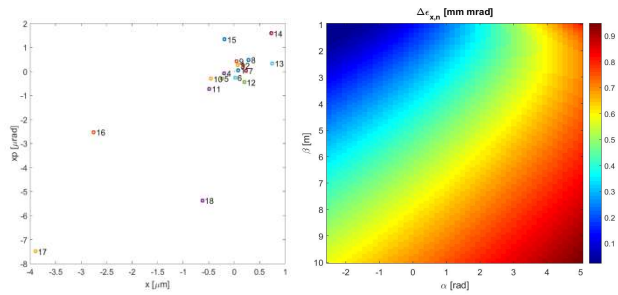

Figure 2: Left: particle transverse displacement in the horizontal phase space due to CSR energy-kicks in the FODO-compressive arc dipoles. The numbers correspond to CSR kicks at the eighteen consecutive dipoles. Right: normalized projected horizontal emittance growth as a function of Twiss parameters at the end of the beamline, calculated with the CSR kick model. Copyright of APS (2017).

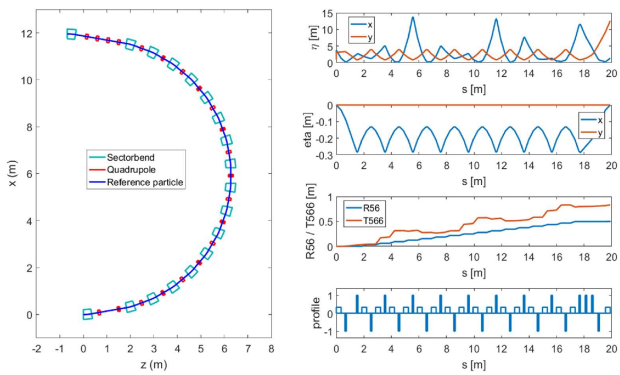

Figure 3: Left: top view of the compressive arc. Right: Optics functions along the arc compressor. From top to bottom: betatron functions, dispersion functions, first and second order transport matrix coefficients, magnetic elements. Copyright of APS (2017).

ISBN: 978-3-95450-206-6 doi:10.18429/JACoW-FLS2018-THA1WC01

COMPACT FEL–ICS

Overview

A sketch of the FEL-ICS light source is shown in Fig.4 and the main parameters are listed in Tab.2. Unlike a standard ICS light source driven by the interaction of an electron beam with an external laser, in the FEL-ICS approach the electron beam interacts with its own UV radiation produced in an undulator. This scheme provides a stronger scaling of the scattered photon energy with the electron beam energy (fourth power instead of the standard square law) [3]. The stronger scaling law involves a lower electron beam energy for a target photon energy, thus a shorter linac for a given accelerating gradient. In addition, coherent UV photon pulses and gamma rays are simultaneously provided for experimentation. The arc provides longitudinal compression to the incoming electron bunches in order to drive the FEL into the high gain regime with a relatively high peak current at the undulator, reducing its gain length while avoiding additional magnetic insertions (e.g., chicanes). As in the case of the ERL-FEL a moderate compression factor has to be obtained while keeping the beam energy spread, and therefore the linear energy chirp, quite low, as requested by efficient lasing in the undulator. For this reason, a relatively large R_{56} is desired (Tab.2). The arc extension determines the FEL-ICS transversal footprint and contributes to the overall length via the loop extension for a given value of the interaction angle at the IP.

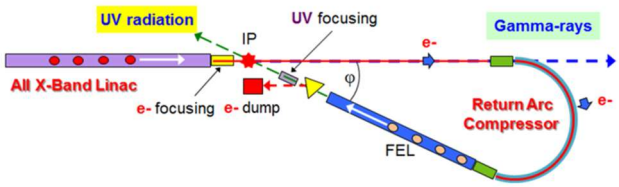

Figure 4: FEL-ICS scheme involving an electron beam return compressive arc. Two photon energies, UV and gamma-rays, are simultaneously available to experiments. Quadrupole triplets provide overlap control at the interaction point (IP) and beam properties matching for arc and undulator. The return arc provides longitudinal bunch compression for improved FEL performance. The system footprint is about 22x4 m^2.

Table 2: FEL-ICS Parameters

Parameter	Value	Unit
Bunch Charge	350	pC
Initial Bunch Duration	2.8	ps
Initial Proj. Norm. Emittance	0.5, 0.5	μm
Final Energy	0.3	GeV
Final Peak Current	0.5	kA
Final Relative Energy Spread	< 0.2	%
FEL Wavelength	150	nm
FEL Peak Power	0.7	GW
Arc Compression Factor	15	
Arc R_{56}	0.2	m
Proj. Norm. Emittance Growth	< 0.3	μm

Arc Compressor

Scaling of the ERL-FEL FODO-cell arc compressor (see previous Section) to the beam energy of 0.3 GeV implies a reduction of the arc length by approximately a factor 3. Since the CSR energy kick is inversely proportional to the beam energy, additional focusing along the arc is needed with the aim at controlling the emittance growth along the line at such reduced beam rigidity, as well as a higher bunch charge. Unlike the ERL-FEL arc compressor, sextupole magnets are added here for linearization of the compression process, while geometric and chromatic aberrations are partially compensated by a suitable arrangement of the sextupoles' location and strength, optimized through `elegant` tracking runs. The magnet list is collected in Tab.3. Figure 5 shows the linear optics functions (top plot), bunch length and transverse emittances along the arc as predicted by the `elegant` code.

Table 3: FEL-ICS Magnets

Type (Quantity)	Field / Gradient	Length
Dipole (7)	1.2 T	0.4 m
Quadrupole (21)	< 60 T/m	0.1 m
Sextupole (4)	< 200 T/m^2	0.1 m

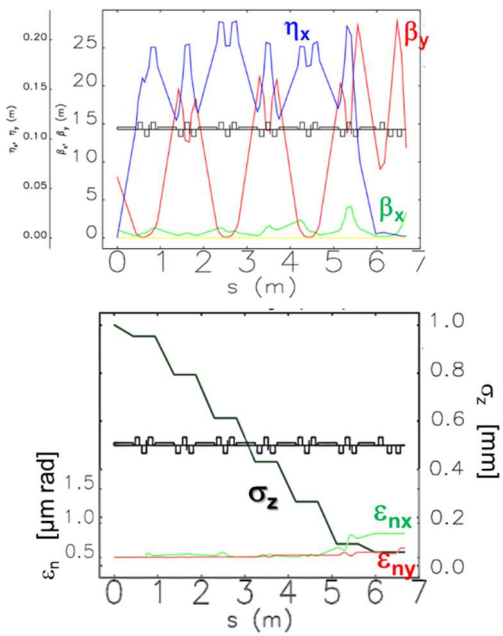

Figure 5: Top, linear optics functions along the FEL-ICS arc compressor. Bottom, rms bunch length and transverse normalized emittances along the arc.

Microbunching Instability

Because of the relatively low beam energy and large bending angle, CSR tends to modulate the beam distribution at wavelengths in the micron range, i.e., CSR drives broadband microbunching instability whose gain appears to be peaked at ~1 μm; energy and density modulations excite reciprocally through the particles' dispersive mo-

ISBN: 978-3-95450-206-6 doi:10.18429/JACoW-FLS2018-THA1WC01

tion. Elegant tracking run, although still affected by numerical sampling noise, reveals a not negligible modulation of the peak current profile at the arc exit, as shown in Figure 6. This effect is not yet consistently treated in the UV FEL simulation, although a preliminary estimation of the FEL performance in the presence of enlarged slice energy spread does not reveal any show stopper.

Recently, optics prescriptions to build up multi-bend *isochronous* transfer lines with unitary microbunching gain were proposed [10], and experimentally verified [11]. Similar treatment might be extended to non-isochronous arcs. It is likely, however, that a compromise shall be reached between the conflicting action of low microbunching gain and large momentum compaction.

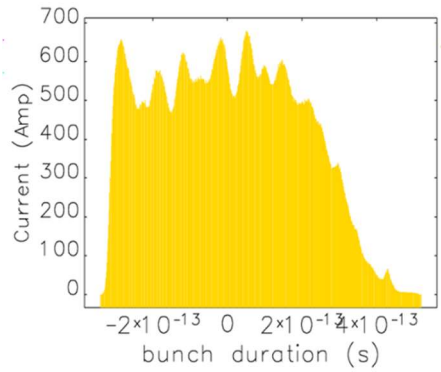

Figure 6: Current profile at arc exit in the presence of CSR-driven microbunching instability.

CONCLUSION

Optics design strategies for two compact arc compressors are illustrated, with application to an ERL-UV FEL devoted to nano-lithography, and to a FEL-based ICS light source devoted to tomography of cultural heritage and medical diagnostics. An approximated analytical calculation of CSR effect on the projected normalized emittance (in the bending plane) in the presence of an arbitrary number of dipoles is illustrated, whose accuracy of prediction w.r.t. 1-D tracking codes appears to be at level of 0.1 μm rad. The analytical guideline might be considered as a first step in arc compressors design, further processed by, e.g., MOGA-like algorithms. This study reveals the appearance of relatively strong microbunching instability in a return arc at beam energies lower than few hundreds of MeV. Minimization of microbunching gain and simultaneous preservation of transverse emittance can be achieved in isochronous lines. Obtaining similar result in arcs with large momentum compaction remains an open path of research.

ACKNOWLEDGEMENT

M. Cornacchia, P. Smorenburg, C.-Y. Tsai, B. Van der Geer, P. Williams and A. Brynes are acknowledged for insights on modelling of CSR and MBI instability.

REFERENCES

[1] Ya.S. Derbenev, J. Rossbach, E.L. Saldin and V.D. Shiltsev, "*Microbunch radiative tail-head interaction*", in *Proc. TESLA-FEL'95*, DESY, Hamburg, Germany (1995).

[2] J. A. G. Akkermans, S. Di Mitri, D. Douglas, and I. D. Setija, "Compact compressive arc and beam switchyard for energy recovery linac-driven ultraviolet free electron lasers", *Phys. Rev. Accel. Beams,* vol. 20, p. 080705, 2017.

[3] M. Placidi, S. Di Mitri, C. Pellegrini, G. Penn, "Compact FEL-Driven Inverse Compton Scattering Gamma-Ray Source", *Nucl. Instr. Meth. A*, vol. 855 (2017).

[4] E. L. Saldin, E. A. Schneidmiller, and M. V. Yurkov, "On the coherent radiation of an electron bunch moving in an arc of a circle", *Nucl. Instr. Meth. A* , vol. 398, p. 373 (1997).

[5] S. Di Mitri, M. Cornacchia, and S. Spampinati, "Cancellation of Coherent Synchrotron Radiation Kicks with Optics Balance", *Phys. Rev. Lett.*, vol. 110, p. 014801 (2013).

[6] S. Di Mitri and M. Cornacchia, "Transverse emittance-preserving arc compressor for high-brightness electron beam-based light sources and colliders", *Europ. Phys. Letters*, vol. 109, p. 62002.

[7] M. Borland, "elegant: A Flexible SDDS-Compliant Code for Accelerator Simulation", *Advanced Photon Source*, LS-287 (2000).

[8] S. Di Mitri , N. Adhlakha, P. Di Pietro, S. Nicastro, A. Perucchi, E. Roussel, S. Spampinati, M. Veronese, E. Allaria, L. Badano, G. De Ninno, B. Diviacco, G. Gaio, D. Gauthier, L. Giannessi, G. Penco, P. Rebernik, C. Spezzani, M. Trovo', "*Coherent THz Emission Enhanced by Coherent Synchrotron Radiation Instability*", to be published.

[9] S. Di Mitri, "Feasibility study of a periodic arc compressor in the presence of coherent synchrotron radiation", *Nucl. Instr. Meth. A*, vol. 806 (2015).

[10] C.-Y. Tsai, S. Di Mitri, D. Douglas, R. Li, and C. Tennant, "Conditions for coherent-synchrotron-radiation-induced microbunching suppression in multibend beam transport or recirculation arcs", *Phys. Rev. Accel. Beams*, vol. 20, 024401 (2017).

[11] S. Di Mitri and S. Spampinati, "Microbunching instability study in a linac-driven free electron laser spreader beam line", *Phys. Rev. Accel. Beams*, vol. 20, 120701 (2017).